

# Rehydration and Rehydroxylation in Ancient Ceramics: New Constraints from Mass Gain Analyses Versus Annealing Temperatures

Yves Gallet and Maxime Le Goff<sup>†</sup>

Institut de Physique du Globe de Paris, Sorbonne Paris Cité, Univ. Paris Diderot, CNRS, Paris F-75005, France

We present a series of new mass-gain data acquired on ancient pottery following heating at increasing temperatures from 60°C to 590°C to further constrain our understanding of the rehydration and rehydroxylation (RHX) processes acting within archeological fired-clay artifacts. The ancient pottery, deliberately chosen for its low-porosity, is second century AD Samian ware fragments originating from Lezoux in central France. The mass-gain data, after each temperature step, adequately define a  $(\text{time})^{1/N}$  power law. We demonstrate that values of the  $1/N$  exponent vary systematically with heating temperature. These results suggest that the sorption of chemisorbed and rehydroxylated water into the clay matrix occurs simultaneously. The  $1/N$  exponent values obtained are consistent with power law kinetics resulting from the combination of both one-dimensional and Brownian diffusion processes. The balance between these two end-member processes, in particular after heating at 500°C, may depend on the nature of the clay and on the manufacturing conditions of the studied ceramics. The results presented herein confirm previous claims that major complexities vitiate the RHX dating method proposed by Wilson et al.<sup>1</sup>

## I. Introduction

SINCE the description of the rehydroxylation (RHX) dating method by Wilson et al.,<sup>1</sup> several groups around the world have failed in their attempt to apply this original method to the dating of archeological fired-clay artifacts of various ages and from different geographical regions. Instead, these studies revealed several complexities bringing into question certain fundamental aspects of the method (e.g., Refs. [2–9]) and more broadly the state of our understanding of the kinetics of rehydration and RHX processes acting in ceramics after their firing.

One fundamental aspect concerns the uncertainty surrounding how the archeological mass of the samples is specified, which is critical since this mass is used as a reference to determine the age of the samples in the laboratory RHX experiments. According to Wilson et al.,<sup>1</sup> the reference mass is obtained by drying the sample at 105°C and then from its continuous weighing in a climatic chamber in constant temperature and relative humidity (RH%) conditions over a period of a few days. The sample mass should first increase rapidly, mainly reflecting a mass gain by capillary action, before reaching, after 1–2 d, a constant value that defines the archeological mass. From the study of more than one hundred different samples, Le Goff and Gallet<sup>6,7</sup> showed that the sample mass never reaches a stable value as required by the Wilson et al.<sup>1</sup> protocol. Instead the observation is that after

a period of rapid mass gain, the sample mass appears to follow a slow diffusion-like process, with a gradual and continuous increase.

A second critical aspect concerns the fundamental condition of the RHX dating method, that is, the power law in  $(\text{time})^{1/4}$  reflecting the (re)hydroxylation process that would strictly obey the long-term mass evolution of fired-clay ceramic samples after their heating at high temperature (>500°C) (e.g., Refs. [1, 9–13]). Both Bowen et al.<sup>2,3</sup> and Le Goff and Gallet<sup>6–8</sup> argued that the  $1/4$  exponent of the power law is far from being experimentally ascertained. In particular, Le Goff and Gallet<sup>8</sup> reanalyzed the data reported by Hall et al.<sup>13</sup> from which the observation of the  $t^{1/4}$  kinetic law for the (re)hydroxylation process in ceramics (mass gain and moisture expansion) was founded. They showed that the best estimate, in the mean-squared sense, of the  $1/N$  exponent varies significantly and is dataset dependent,<sup>10,14–17</sup> ranging from  $1/2$  (i.e., a Brownian diffusion) to  $1/4$  (a one-dimensional diffusion process (e.g., Ref. [12] and references therein).

The results above highlight the interest in further investigating the rehydration and RHX processes in ancient fired-clay ceramics along the lines of the principles of the RHX dating method. In this study, we carried out a series of mass-gain measurements directly associated with these processes after heating ceramic fragments at increasing temperatures. One point that seems important for these analyses is the choice of Samian ware fragments characterized by very low porosity. By reducing the amount of water gained by capillary action, one can better observe the diffusion processes involved in chemical water sorption.

## II. Sample Description

In this study, we used fragments of Samian ware produced in Lezoux (central France), which was a major center of pottery production during the Roman Empire (e.g., Refs. [18,19]). The fragments were found in the same pit excavated inside the retirement residence “Mon Repos” (archeological reference, OA6996; Philippe Bet, pers. comm.). According to their typology and decor, they are dated to between 160 and 190 AD, that is, the period encompassing the reign of Emperors Marcus Aurelius (161–180 AD) and Commodus (180–192 AD). These fragments correspond to ceramics thrown out in the vicinity of the kiln where they were originally fired, most probably because the temperature reached during the firing exceeded the normal temperature (i.e., ~950°C–1000°C [Ref. 20]). This excess in temperature induced a change from the usual orange-red to a wine lees color indicating a firing temperature between 1000°C and 1100°C [Ref. 20]. As previously mentioned, we made the choice of Samian ware fragments for our experiments because previous studies have shown the waterproof nature of this type of ceramics, with a vitrified pore structure due to the high firing temperature, and thus the large insensitivity of their mass evolution to eventual small changes in humidity during laboratory experiments.<sup>6,11</sup> We further note that the fragments analyzed in this study are different from

W. Lee—contributing editor

those analyzed in Le Goff and Gallet<sup>6</sup> (different ages and different archeological contexts).

Five fragments (LEZ01-01; LEZ01-02; LEZ01-06; LEZ01-09; LEZ01-18) from different pots were selected on the basis of the excellent stability of their magnetic mineralogy on heating at high temperature (500°C; see discussion in Le Goff and Gallet<sup>6,7</sup>). Furthermore, X-ray powder diffraction (XRD) analyses were carried out on the fragments in order to identify the different mineral phases, excluding, however, the vitreous phases. All fragments reveal the same composition, dominated by anorthite, albite, quartz, and hematite (see the inset in Fig. 1). For two fragments (LEZ01-06 and LEZ01-09), diffraction patterns were obtained from three samples, one which was not heated in the laboratory, a second heated at 500°C and a third sample heated at 590°C (i.e., respectively after the laboratory experiments conducted in this study, see below). In both cases, no mineralogical changes were detected in response to laboratory heating at 500°C for 96 h or up to 590°C for 92 h (Fig. 1). The XRD results cast aside any speculation of mass changes due to progressive mineral alteration and unequivocally attest to mass-gain behaviors described hereafter being solely due to rehydration- RHX kinetics as a function of the annealing temperatures.

### III. Experimental Procedure

Each of the five fragments was cut into four sister samples to form two sets of twins referred below to as [a], [b] and [c], [d]. The cylindrical samples have a diameter of 12 mm and maximum heights of 15 mm. Their masses range from ~1.46 to ~3.0 g. The ancient surfaces of the fragments were carefully removed from all samples to avoid spurious effects due to possible surface alteration. Mass measurements were carried out using the device described by Le Goff and Gallet.<sup>6</sup> We briefly recall that thanks to a rotating carousel, this instrument allows the automatic weighing of 10 samples in one series of experiments under controlled (and constant) temperature and relative humidity conditions. Here, these conditions were arbitrarily chosen at 13°C and 33% RH. Moreover, the climatic chamber possesses an airlock system permitting the addition and removal of samples to the rotat-

ing carousel, without noticeable perturbations to the prescribed temperature and humidity of the chamber.

The different series of weighing lasted for at least 90 h (almost 4 d), a duration always longer than that previously used by Ince.<sup>21</sup> It is worth reminding that the data obtained by Ince,<sup>21</sup> also reported in Wilson et al.,<sup>1,11</sup> constitute the bulk of successful RHX dating results achieved so far. The first series of 10 samples (LEZOUX-04) was analyzed using the longest durations for each step: drying at 105°C for 246 h (10 d), weighing over 142 h (6 d), high-temperature (500°C) firing for 96 h (4 d) and subsequent weighing for 720 h (30 d).

The second series of 10 samples (LEZOUX-05) was analyzed in a progressive manner as follows:

1. Samples [c] were first dried at 105°C for 23 h, whereas samples [d] were placed in a desiccator for 6 h.
2. Samples [c] and [d] were next weighed together over 91 h (~3.1 h<sup>1/2</sup>).
3. Samples [d] were regularly removed from the climatic chamber through its small airlock system,<sup>6</sup> to be gradually heated for 5 h at increasing temperatures and subsequently weighed for 90 h (sometimes longer) after each firing (Fig. 2). Ten heating steps were applied: 60°C, 85°C, 105°C, 130°C, 180°C, 250°C, 350°C, 440°C, 500°C, and 540°C (including an additional heating at 60°C for 5 h after the firing at 180°C, whose results will not be discussed further below because they do not provide additional insight into the behavior reported in the present study). Samples [d] were thus gradually heated over 55 h.
4. After heating (and weighing) of [d] samples at 180°C and 60°C, the [c] samples, which were continuously weighed until then, were regularly removed from the climatic chamber and successively heated at 450°C, 500°C, 550°C, and 590°C over 23 h per step.

### IV. New Results

Figure 2 shows the fractional mass variations, in ppm relative to the initial mass, obtained for the 10 [c] and [d] samples after gradually heating them to 180°C. In all cases, there

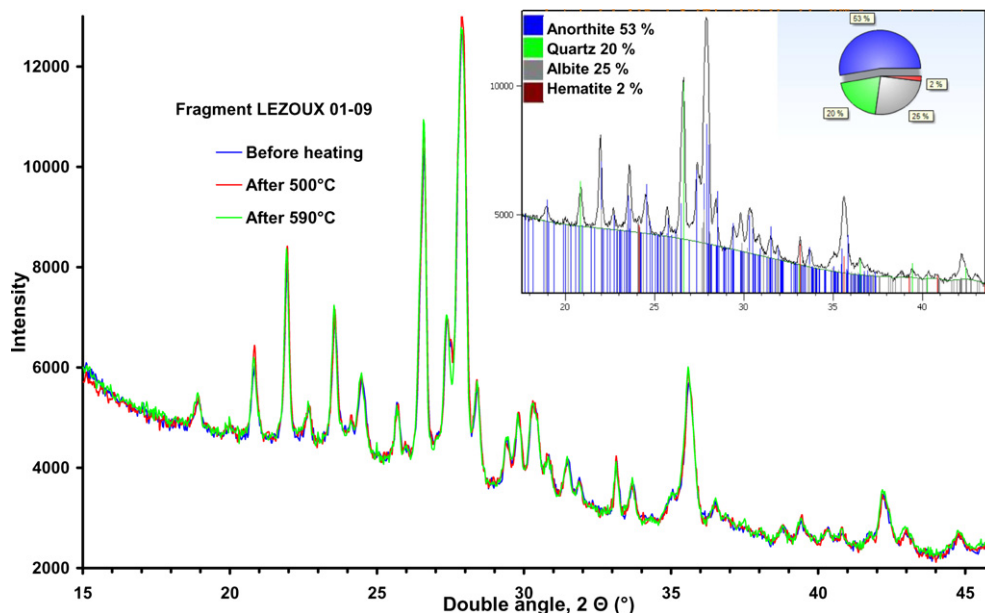


**Fig. 1.** X-ray powder diffraction patterns obtained for fragment LEZ01-09 using an Empyrean-Panalytical diffractometer (XRD instrumental platform at Paris Diderot University). This instrument was run with a potential difference of 45 kV and a current of 40 mA, and with a copper target ( $\lambda = 1.540598$  Å). The angular range was chosen between 15° and 90° with a step size of 0.0263° (100 s per step). The inset shows the diffraction patterns for a sample not heated in the laboratory. A color code indicates the identified mineral phases and their proportion. The main figure shows a comparison between the diffraction patterns obtained from three samples before and after their heating in laboratory (at 500°C for 96 h and up to 590°C for 92 h).

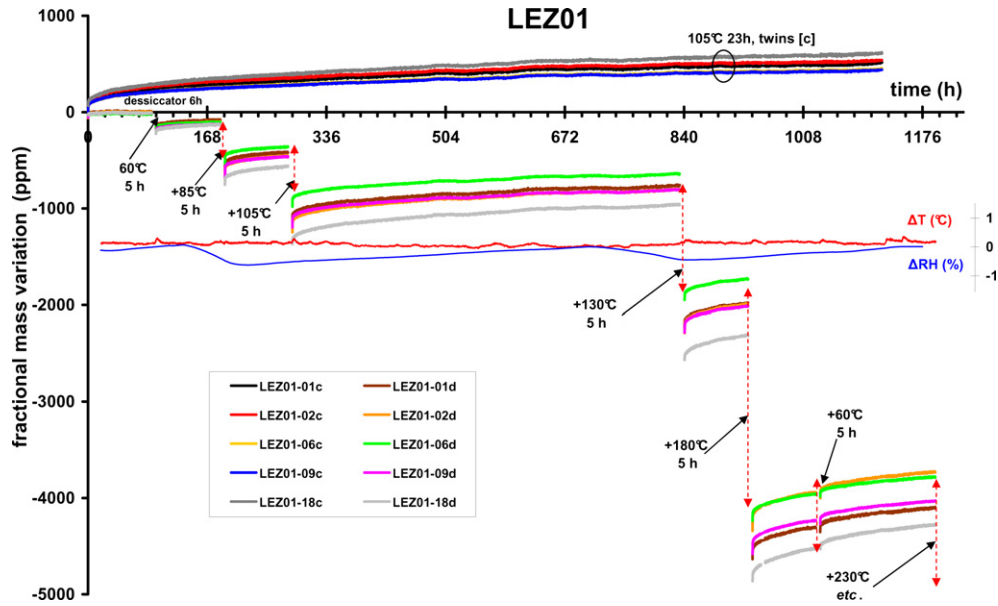


**Fig. 2.** Illustration of the successive rehydration and rehydroxylation experiments performed to study the effect of heating temperature on mass-gain behavior. Five pairs of twin samples were simultaneously weighed (labeled c and d; see code on the figure). Samples [c] were heated once at 105°C for 23 h, whereas samples [d] after desiccation for 6 h were progressively heated up to 540°C (for a better readability, Fig. 2 only displays the results obtained up to 230°C). The reported results are the fractional mass gain data relative to  $m_{RX}$  derived for each sample after the first 92 h of weighing (see text and Le Goff and Gallet<sup>6</sup>). Time (in h) is segmented in weeks (major ticks) and days (minor ticks). The thin blue and red curves, respectively, show the variations in temperature ( $\sim 13^\circ\text{C}$ ) and relative humidity ( $\sim 34\%$ ), which occurred during the experiments. See text for further explanation.

is a loss of mass after each heating, whose amount decreases after each successive firing (see below). During our experiments, the environmental conditions remained stable. In particular, very limited variations ( $\sim 0.5\%$ ) in RH% clearly had no noticeable effect on the mass evolution. Figure 3 displays the fractional mass gain (fmg) data obtained from the four twin samples collected from only one fragment (LEZ01-01). Given the fact that the observed mass-gain behavior is very similar to that due to RHX (e.g., Refs. [6,7]), the fmg data were reported against  $\text{time}^{1/4}$ . For each curve, the fmg is relative to  $m_{RX}$ , that is, the mass derived at  $\text{time}^{1/4} = 0$  from the regression line computed between  $2 \text{ h}^{1/4}$  and  $3.1 \text{ h}^{1/4}$  (i.e., between 16 and 92 h).

We observe the following characteristics:

1. Sample mass steadily increases upon the first heating, even at 60°C.
2. The mass-gain data obtained after three different durations of drying at 105°C indicate that the influence of heating duration on the slope of the fmg curves is negligible, as is also the influence of the weighing duration (the curves obtained from the four sister samples are almost identical).
3. The change in slope around 105°C is significant, between 33 and 42 ppm/°C.
4. The RHX curves clearly display a concavity after heating at 130°C and above.
5. Independent of the mass variation levels, the curves become similar, almost stabilized above 450°C.

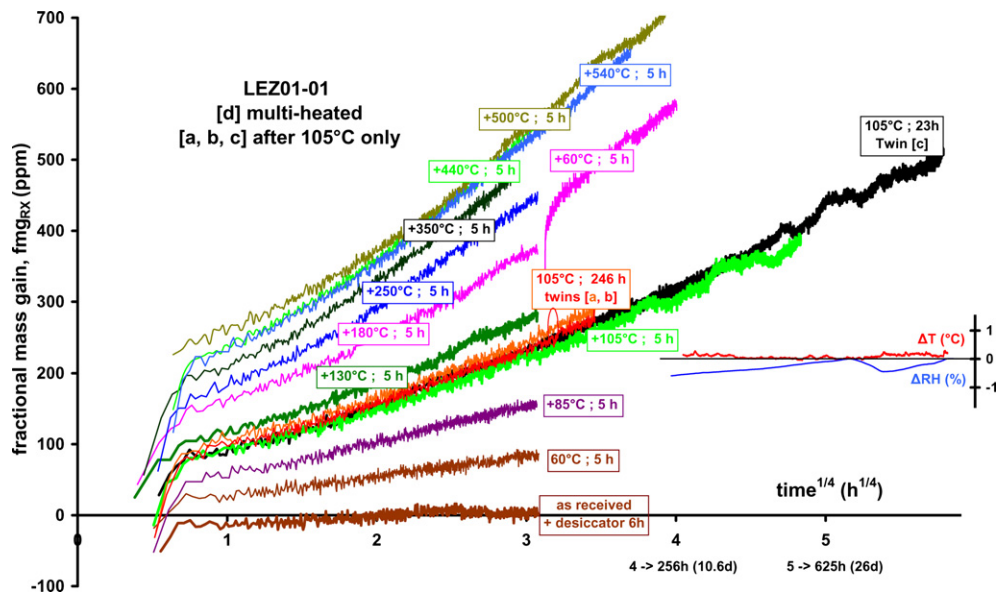


**Fig. 3.** Series of mass-gain data obtained after successive heating, whose corresponding temperature and duration are indicated in small insets (same color code). The fmg data, with  $m_{RX}$  calculated in all cases using the mass-gain data obtained between 16 and 92 h ( $2$  and  $3.1 \text{ h}^{1/4}$ ), are reported against  $\text{time}^{1/4}$ . The thin red and blue curves, respectively, display the changes in temperature ( $\sim 13^\circ\text{C}$ ) and relative humidity ( $\sim 34\%$ ) associated with the black fmg curve (twin [c]) over the same time interval.

Figure 4 exhibits the fmg curves (against  $\text{time}^{1/4}$ ) for the [c] samples from fragments LEZ01-02 and LEZ01-06 after their heating above  $440^\circ\text{C}$ . If the sample from LEZ01-06 shows a certain, though imperfect stability in behavior at these high temperatures (which is generally the case for the three other fragments), the sample from LEZ01-02 reveals a divergent behavior after heating at  $590^\circ\text{C}$ .

Figure 5 presents a synthesis of all the previous results. Figure 5(a) summarizes the observations on the fmg slopes, which were calculated between 2 and  $3.1 \text{ h}^{1/4}$  for ease of comparison. Figure 5(b) illustrates the steady mass loss on heating, as well as the good level of consistency between twin samples even though they experienced different heating sequences. The essential observation is that the data at  $105^\circ\text{C}$  exhibit no peculiarity, being part of a broad smooth evolution between no heating and  $\sim 180^\circ\text{C}$ . The mass variations at or around this temperature, which should be null to provide the reference mass in the RHX dating method, are very significant. They range between 33 and  $42 \text{ ppm}/^\circ\text{C}$ , that is,  $\sim 1\%$  of difference over  $2^\circ\text{C}$  with a  $(m_A - m_{\text{RHX}})$  value of  $\sim 8000 \text{ ppm}$ . This would induce a difference of  $\sim 4\%$  in derived RHX dating results regardless of other uncertainties. Finally, the changes in concavity clearly seen in the fmg curves from Fig. 3 enabled us to determine the  $1/N$  exponent of the  $(\text{time})^{1/N}$  power law that offers the best mean-squared adjustment to each curve. As in Le Goff and Gallet,<sup>6</sup> we used the Levenberg–Marquardt method for these computations, whose results are reported in Fig. 5(c). Note that for consistency, all series were adjusted for exactly the same time interval, that is, between 1.5 and  $3.1 \text{ h}^{1/4}$  (i.e., between 5 and 92 h). Figure 5(a) shows a rather smooth evolution of  $1/N$  as a function of temperature, with 2 maxima at  $\sim 180^\circ\text{C}$  and  $\sim 500^\circ\text{C}$  and a minimum around  $300^\circ\text{C}$ . We further note that  $1/N$  is almost always significantly different from  $1/4$ .

## V. Remarks on the Results

The data reported in this study shed new light on two major complexities in the RHX dating method proposed by Wilson et al.<sup>1</sup> In particular, they illustrate the fact that the archeological mass, a pivotal parameter in this method, cannot be defined after heating the samples at  $105^\circ\text{C}$  (see also Refs. [6,7]). Any heating, even at a temperature as low as  $60^\circ\text{C}$ , induces a systematic long-term increase in sample mass, which resembles a diffusion process. A mass stabilization is only

achieved with a simple desiccation (Fig. 3; see also supplemental Fig. S1 for a similar behavior observed from different samples). Furthermore, the new data make it clear that the mass-gain behavior after heating at  $105^\circ\text{C}$  is part of a broader evolution with a progressive increase in the  $1/N$  exponent between no heating (desiccation) and  $\sim 180^\circ\text{C}$  [Fig. 5(c)].

Another important result is that the mass gain behaviors associated with rehydration/RHX processes appear to reasonably obey a  $(\text{time})^{1/N}$  power law after heating at each temperature step. However, the  $1/N$  exponent systematically varies with heating temperature between 0 with no heating (desiccation) and  $\sim 1/2$  when heating around  $200^\circ\text{C}$  and  $500^\circ\text{C}$ . Values closest to  $1/4$  are obtained around  $100^\circ\text{C}$  and  $300^\circ\text{C}$ .

For the sake of the discussion below, it is also worth recalling that there are three different types of water sorption involved in rehydration/RHX experiments, referred to as T0, T1 and T2 by Wilson et al.<sup>1,11</sup> (see also Refs. [22–24]):

1. T0 or physisorbed water ( $\text{H}_2\text{O}_{\text{phys}}$ ) corresponds to molecules of water rapidly trapped in the pores and cracks of the material, mainly by capillary action and/or van der Waals interaction, and which do not chemically interact with the medium. The mass of gained T0 thus depends on the quantity of free cavities/sites in the material and also on the water partial pressure in the surrounding atmosphere (RH%), which is a function of temperature. Again note that this water component is likely to be extremely weak in our Samian ware samples, which have vitrified pores. The sorption of physisorbed water, which defines “Stage I” of Wilson et al.,<sup>10</sup> was assumed to follow a transient  $t^{1/4}$  kinetic law over a few days at most.<sup>12</sup> Like in a sponge, however, this phenomenon has a physical limit (which is indeed observed after several hours of rapid increase in weight or volume). For this reason, as mentioned by Le Goff and Gallet<sup>6</sup> and according to Bowen et al.,<sup>2</sup> the sorption of T0 is best described by the Lagergren<sup>25</sup> equation, with a time constant that explicitly introduces its saturation. The physisorbed water is rapidly eliminated by moderate heating (drying) above its boiling point (around  $105^\circ\text{C}$ ), and one can thus easily realize that Stage I is reversible and transient.
2. The T1 water component refers to molecular chemisorbed water ( $\text{H}_2\text{O}_{\text{chem}}$ ) still existing in the medium after heating at  $105^\circ\text{C}$ . Its complete removal requires

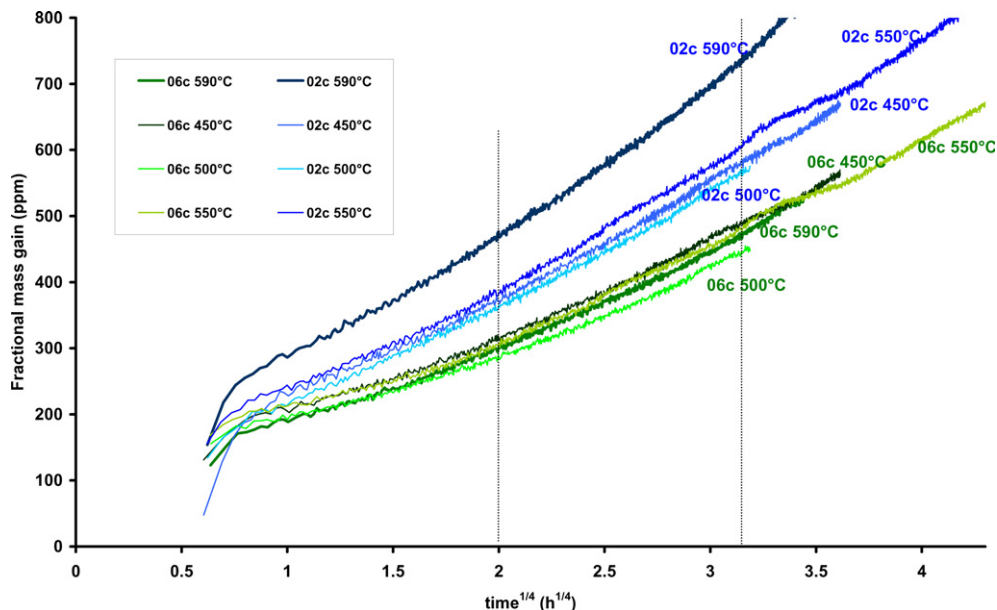


**Fig. 4.** Rehydroxylation curves in  $\text{time}^{1/4}$  obtained for two samples [c] after their heating at four different temperature steps  $>440^\circ\text{C}$  (see color code on the figure). The vertical dotted lines give the time range between 2 and  $3.1 \text{ h}^{1/4}$  used in all cases for our linear-regression estimates (see text for further explanation).

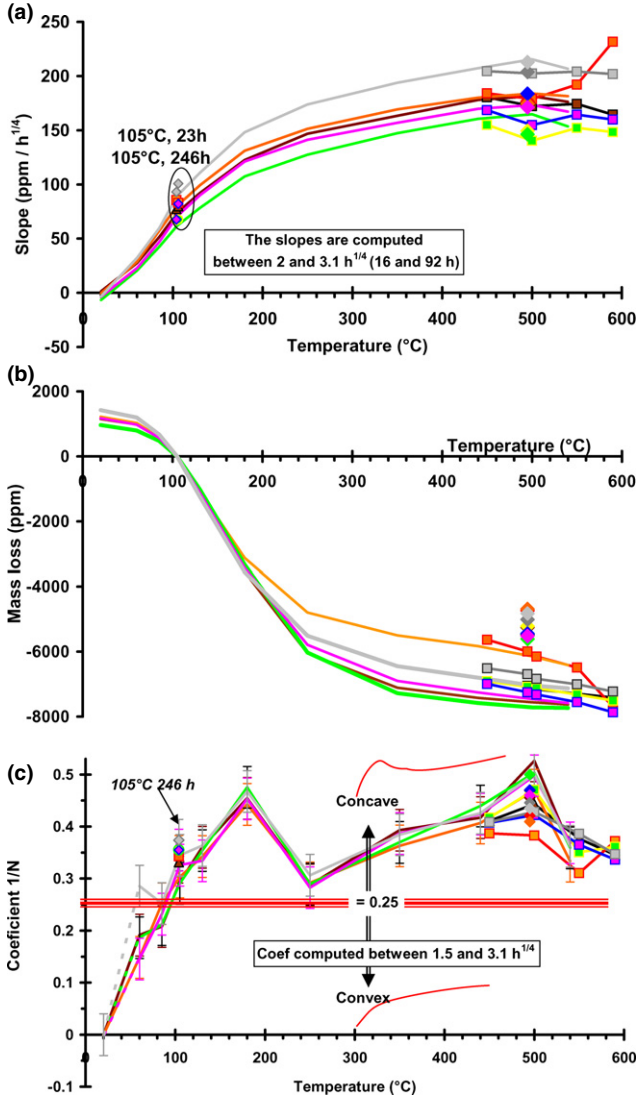


**Fig. 5.** Synthesis of the new data as a function of temperature obtained in this study. (a) Temperature dependence of the slopes of the regression lines estimated in time<sup>1/4</sup>. (b) Temperature dependence of the mass lost after each heating temperature step. The mass of reference is  $m_{RX}$  obtained after heating at 105°C. (c) Temperature dependence of the  $1/N$  exponent in the time<sup>1/N</sup> power law best fitting the data after each heating temperature step (see text for further explanation). Same color code as in Fig. 2 (also the pairs of twin samples [a, b] and [c, d] have the same color). Note that the continuous lines drawn from the discrete data help to better illustrate the progressive effects due to the increase in the heating temperature steps. To ease comparisons with data from samples [d], symbols with the same color are added to the curves obtained at high temperatures from twin samples [c]. The data encircled in an oval in Fig. 5(a) are obtained from samples [a] and [b] after a single heating at 105°C

heating up to  $\sim 300^\circ\text{C}$  (e.g., Ref. [22]). According to Drits and McCarty,<sup>22</sup> this water component “*originates from H<sub>2</sub>O molecules bonded to the outer surfaces and within the interlayers of the mineral structures*”, whereas Wilson et al.<sup>9</sup> favor the following description “*physicochemical bonding of water (weak chemical bonds and water interacting only via hydrogen bonds forming with hydroxyl groups on the surface of the ceramic matrix)*”. But nothing is said about the kinetics governing the gain of H<sub>2</sub>O<sub>chem</sub> into the samples during laboratory experiments, only that the process is reversible and that together with T0, T1 forms the water component T01 involved in (re)hydration.<sup>11</sup> There is no element that excludes the idea that the gain of H<sub>2</sub>O<sub>chem</sub> follows a diffusion process different from that

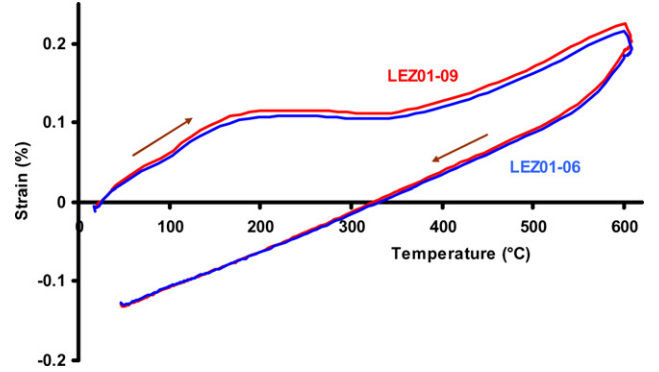


**Fig. 6.** Dilatometry results (% expansion strain) obtained for two samples from fragments LEZ01-06 (blue) and LEZ01-09 (red) using a LINSEIS L75 vertical Dilatometer. The heating was performed in air and static atmosphere up to 600°C, and the heating rate was 10°C/min.

of H<sub>2</sub>O<sub>phys</sub> and of the hydroxyl groups (T2, see below). In our Samian ware samples from Lezoux, the presence of chemisorbed water can be traced up to  $\sim 300^\circ\text{C}$  by dilatometry experiments. Changes in the length induced by heating of two samples from fragments LEZ01-06 and LEZ01-09 were continuously monitored up to 600°C, using a heating rate of 10°C/min (Fig. 6). Below  $\sim 300^\circ\text{C}$ , the results clearly show a bump with an apparent contraction of the medium between  $\sim 180^\circ\text{C}$  and  $\sim 300^\circ\text{C}$  (see comparable results in Clegg et al.<sup>24</sup> and Vokác et al.<sup>26</sup>). This behavior is not reversible during cooling, with a curve showing a steady trend towards a contraction. The bump observed during heating can be attributed to the removal of the T1 water component resulting in a contraction of the matrix, which counterbalances the thermal expansion effect over the concerned temperature range. Furthermore, as the T0 water component is practically absent in the waterproof Samian ware samples, it is tempting to link the lack of stabilization of the sample mass we generally observe after heating at 105°C<sup>6,7</sup> with the long-term recovery of chemisorbed water previously removed at this temperature. As a general matter, any heating, even at relatively low temperature, would *de facto* involve the T1 water component and its subsequent long-term recovery during rehydration.

- T2 or H<sub>2</sub>O<sub>rhx</sub> refers to hydroxyl groups involved in the (re)hydroxylation process. The rehydroxylated water bonds within the matrix and its gain over time into the matrix defines “Stage II” of Wilson et al.<sup>1,10</sup> According to Wilson’s team,<sup>1,9–11,27</sup> the gain of H<sub>2</sub>O<sub>rhx</sub> accurately follows a one-dimensional diffusion process, that is a (time)<sup>1/4</sup> power law. From an experimental view point, however, this assertion now seems hardly tenable because the available results clearly show a significant variability in the  $1/N$  exponent values between  $\frac{1}{2}$  and  $\frac{1}{4}$ .<sup>2,6–8</sup> In the case of our samples from Lezoux, the  $1/N$  exponent after heating at 500°C lies much closer to  $\frac{1}{2}$  than to  $\frac{1}{4}$  [Fig. 5(c)]. Let us also recall that Wilson et al.<sup>1,11</sup> assumed that the T2 water component was completely removed from the clay matrix by heating at  $\sim 500^\circ\text{C}$ , but this issue could in fact be more complex. For instance, Bowen et al.<sup>2</sup> showed that heating to higher temperature would be necessary at least in some cases (see also Ref. [22]).

## VI. Discussion

The simple examination of the new data presented in this study points to the existence of major complexities vitiating the RHX dating method proposed by Wilson et al.<sup>1</sup> Beyond this aspect, understanding the  $1/N$  evolution shown in Fig. 5(c)

remains a contentious issue. Apart from the gain of T0 that is clearly a short-term and reversible phenomenon (at constant temperature and RH%) with respect to the mass-gain behavior characterizing T1 and T2, our results suggest that during the RHX experiments T1 and T2 water components are not re-sorbed in succession into the ceramic matrix (i.e., chemisorbed water resorb first followed by rehydroxylated water) but are re-sorbed simultaneously. Furthermore, keeping in mind that archeological ceramics are more or less porous with cavities of varying sizes, we consider the possibility that the sorption of T1 and T2 corresponds to phenomena with simultaneous temporal variations. These combined phenomena would follow power law kinetics consistent with one-dimensional and/or Brownian diffusion processes, depending on the diversity of available voids (cracks, interlayer cavities, etc.) and on the availability after each heating of vacant sites for molecular water and hydroxyl groups.

Using this scheme, the behavior of  $1/N$  displayed in Fig. 5(c) might be explained as follows: up to  $\sim 180^\circ\text{C}$ , a large number of sites previously occupied by natural  $\text{H}_2\text{O}_{\text{chem}}$  are freed [see the important loss of mass after each heating, Fig. 5(b)] and the adsorption of laboratory  $\text{H}_2\text{O}_{\text{chem}}$  becomes more and more efficient (exponent  $1/N$  increases to  $\sim 1/2$ ); between  $\sim 180^\circ\text{C}$  and  $\sim 300^\circ\text{C}$ , the environment progressively

becomes more restricted for the adsorption of this water component because heating at these temperatures allows the release of a too small number of sites previously occupied by natural rehydroxylated water, preventing a significant conversion of weakly bound laboratory  $\text{H}_2\text{O}_{\text{chem}}$  into strongly bound laboratory  $\text{H}_2\text{O}_{\text{rhx}}$  ( $1/N$  decreases to  $\sim 1/4$ ). In contrast, between  $\sim 300^\circ\text{C}$  and  $\sim 500^\circ\text{C}$  the sites occupied by natural rehydroxylated water are progressively freed, allowing the conversion of an increasing quantity of laboratory  $\text{H}_2\text{O}_{\text{chem}}$  into  $\text{H}_2\text{O}_{\text{rhx}}$  and the adsorption of laboratory  $\text{H}_2\text{O}_{\text{chem}}$  therefore becomes again more and more efficient (exponent  $1/N$  approaches  $\sim 1/2$ ). We note that the exponent  $1/N$  may converge toward various values up to  $1/2$  (e.g. Ref. [6]) depending on the type of fired-clay ceramics.

Hence, we propose that the rehydration and RHX processes occurring during laboratory experiments obey the general equation:

$$\text{fmg}(t) = -\beta e^{-t/\tau} + \mu + \alpha_4 t^{1/4} + \alpha_2 t^{1/2} \quad (1)$$

where  $\beta$  is the amplitude and  $\tau$  the time constant of Stage I,  $\alpha_4$  and  $\alpha_2$  are the mass-gain rates for both one-dimensional and Brownian diffusions, and  $\mu$  is the initial fmg at the “beginning” of the reaction (at time  $t = 0$ ).

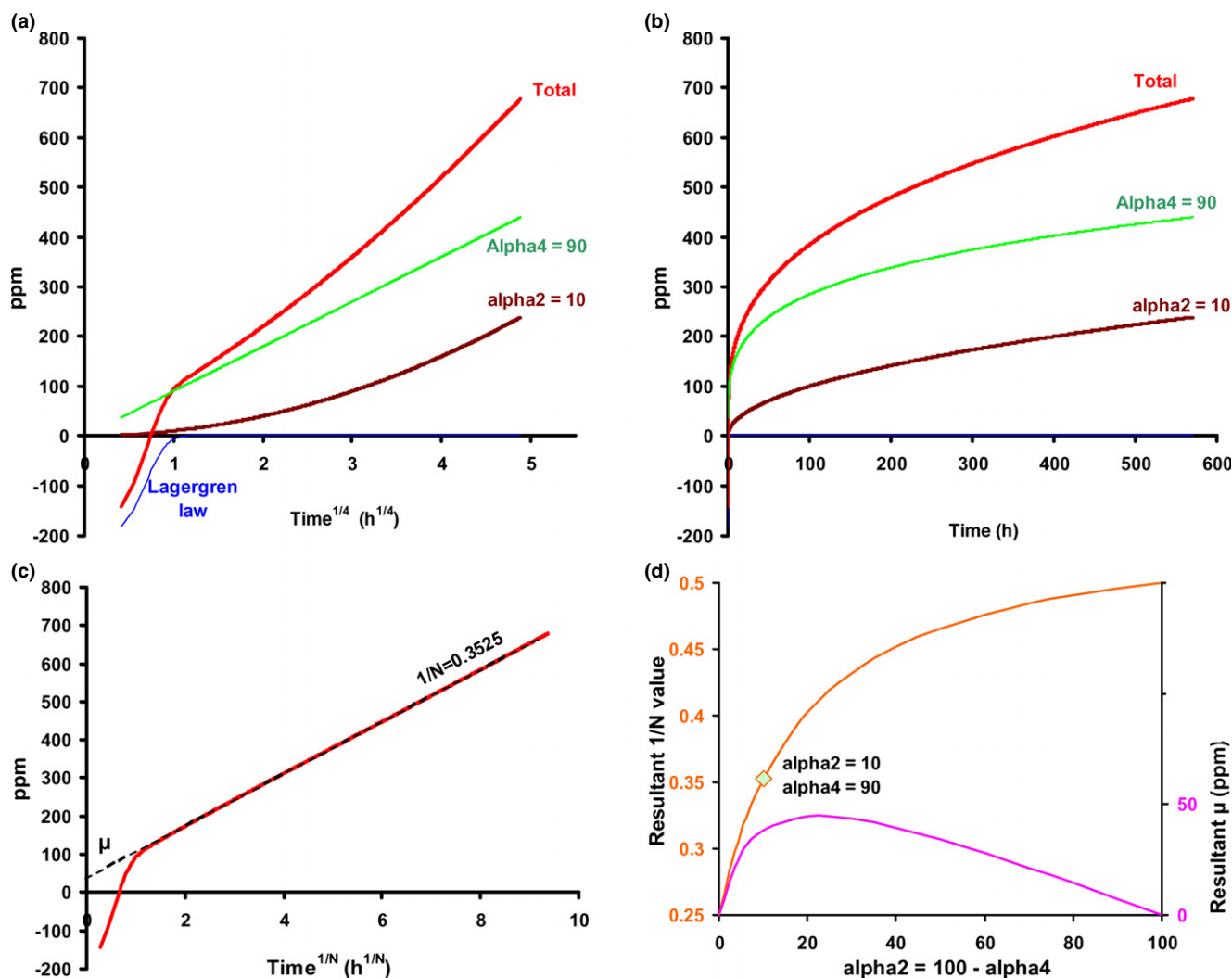


Fig. 7. Synthetic mass-gain variations provided by Eq. (1) from the text. The fractional mass-gain results (in ppm) are successively reported against time in  $\text{h}^{1/4}$  (a) and in h (b). The blue curve shows the fmg variations induced by the rapid sorption of the T0 water component ( $\text{H}_2\text{O}_{\text{phys}}$ ). The magenta (resp. green) curve shows the fmg variations resulting from a  $t^{1/4}$  (resp.  $t^{1/2}$ ) power law diffusion process using an arbitrary coefficient  $\alpha_4$  (resp.  $\alpha_2$ ; see text). The combination of the three processes yields the resultant curve in red. (c) Best fitting of the resultant curve provided by a  $(\text{time})^{1/N}$  power law. In the present case, with  $\alpha_4 = 90$  and  $\alpha_2 = 10$ , the resultant exponent  $1/N$  is 0.3525, defining a  $\mu$  value at time = 0 [see Eq. (1)]. (d) Variations in the resultant exponent  $1/N$  and of the corresponding  $\mu$  value as a function of the relative proportion between the  $t^{1/4}$  and  $t^{1/2}$  law models (left and right scale, respectively).

Figure 7 shows an example of mass-gain evolution produced by Eq. (1). After  $\sim 1 \text{ h}^{1/4}$  (i.e., after the rapid sorption of T0), the mass gain behaves according to the combination of the two  $t^{1/4}$  and  $t^{1/2}$  power law processes. In this example, the first dominates the second [ $\alpha_4 = 90$ ,  $\alpha_2 = 10$ ; green curve and violet curve, respectively in Figs. 7(a) and (b)]. The resultant mass-gain curve (in red) appears very similar to numerous data sets previously obtained by several authors (e.g., Refs. [2,6,7,9,28]) and it can be precisely described by a (time) $^{1/N} = 0.3525$  power law model [Fig. 7(c)]. Supplemental Fig. S2 shows an animation of the resultant curve where the relative proportion between the  $t^{1/4}$  and  $t^{1/2}$  power law processes changes from 0% to 100%. Not surprisingly, Fig. 7(d) further shows that the  $1/N$  exponent value of the resultant power law model varies from  $1/4$  to  $1/2$  as a function of this relative proportion. In reality, it may well be that the combination between these two laws depends on the nature of the clay and on the manufacturing conditions (heating) of the ceramics. Such a simple scenario could therefore explain the variability of the  $1/N$  values determined from RHX experiments.<sup>6,8</sup> However, it is worth mentioning that this empirical scenario still seems a bit simplistic as it cannot explain the few cases where the  $1/N$  exponent is lower than  $1/4$  (e.g., Refs. [6,7,9]).

## VII. Concluding Remarks

The results presented herein confirm previous claims that major complexities and uncertainties vitiate the RHX dating method proposed by Wilson et al.,<sup>1</sup> making its actual application very problematic, not to say impossible, in the present state of knowledge.

Our work leads us to propose a general mass versus time equation that accounts for the majority of the mass-gain results obtained from ancient fired-clay ceramics during rehydration and RHX experiments conducted in the framework of the RHX dating method. In particular, this equation would take into account the variability of the samples, hopefully offering a new avenue of research for this method. Indeed, it is important to continue testing the parameters governing this original clock owing to its exceptional interest for all themes of archeological research, as well as for other related disciplines such as archeomagnetism.<sup>6,29</sup>

## Acknowledgments

We thank Philippe Bet who provided us with the ceramic fragments from Lezoux. We are also grateful to Stuart Gilder and France Lagroix for their helpful reading of the manuscript, and to Sophie Nowak (XRD instrumental platform at Paris Diderot University), Ludovic Delbes and Benoît Baptiste (IMPIC) for the acquisition and interpretation of X-ray diffraction data. This work was supported by IPGP and INSU-CNRS via the PNP program. IPGP contribution no. 3633.

## Supporting Information

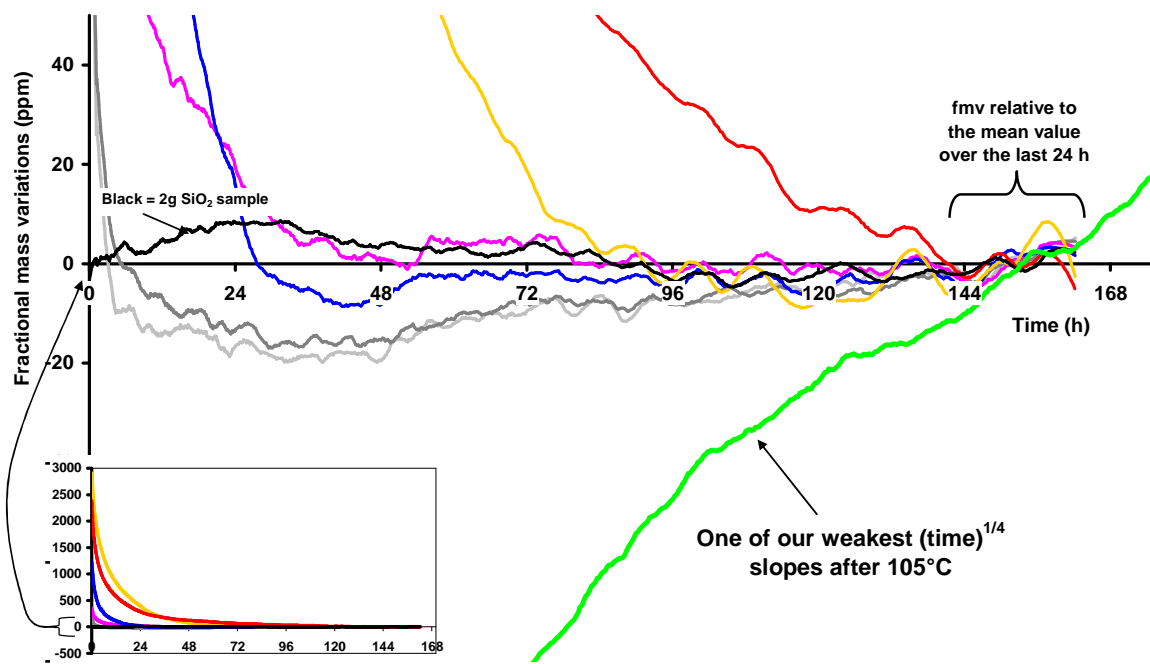
Additional Supporting Information may be found in the online version of this article:

**Fig. S1.** Fractional mass variations (fmv) in ppm at constant temperature (12.6°C) and RH% (32%) obtained for different samples of French fired-clay ceramics during their re-equilibrium after several weeks of “natural” drying (i.e., after their wet cutting) in room conditions (>60% RH,  $\sim 20^\circ\text{C}$ ). Red and yellow curves: samples from site Bois d’Epense -BDE01-, 1785-1815 AD; blue, pink, dark grey and light grey curves: samples from site Ancy-le-Franc -ALF03-, 1797–1807 [see in Le Goff and Gallet, (6)]. The small inset shows the full-scale variations. For comparison, we also show the fmv obtained from an inert sample of SiO<sub>2</sub> (black curve) and the data from a Lezoux fragment [same collection as in Le Goff and Gallet, (6)] showing one of the smallest  $t^{1/4}$  slope after heating at 105°C (green curve).

**Fig. S2.** Animation of resultant mass-gain curves derived from Equation (1) given in the text. Same legend as for Fig. 7, except that the combination between the  $t^{1/4}$  and  $t^{1/2}$  power law processes changes from 0% to 100%.

## References

- M. A. Wilson, et al., “Dating Fired-Clay Ceramics Using Long-Term Power Law Rehydroxylation Kinetics,” *Proc. R. Soc. London, A*, **465**, 2407–15 (2009).
- P. K. Bowen, H. J. Ranck, T. J. Scarlett, and J. W. Drelich, “Rehydration/Rehydroxylation Kinetics of a Reheated XIX-Century Davenport (Utah) Ceramic,” *J. Am. Ceram. Soc.*, **94**, 2585–91 (2011).
- P. K. Bowen, J. W. Drelich, and T. J. Scarlett, “Modeling Rehydration/Rehydroxylation Mass-Gain Curves from Davenport Ceramics,” *J. Am. Ceram. Soc.*, **96**, 885–91 (2013).
- K. S. Burakov and I. Nachasova, “Archeomagnetic Study and Rehydroxylation Dating of Fired-Clay Ceramics,” *Izvestiya Phys. Solid Earth*, **49**, 105–12 (2013).
- S. Shoval and Y. Paz, “A Study of the Mass-Gain of Ancient Pottery in Relation to Archeological Ages Using Thermal Analysis,” *Appl. Clay Sci.*, **82**, 113–20 (2013).
- M. Le Goff and Y. Gallet, “Evaluation of the Rehydroxylation Dating Method: Insights from a New Measurement Device,” *Quat. Geochronol.*, **20**, 89–98, doi: 10.1016/j.quageo.2013.12.001 (2014).
- M. Le Goff and Y. Gallet, “Evidence for Complexity in the RHX Dating Method,” *Archaeometry*, doi: 10.1111/arc.12137 (2015).
- M. Le Goff and Y. Gallet, “Experimental Variability in Kinetics of Moisture Expansion and Mass Gain in Ceramics,” *J. Am. Ceram. Soc.*, **98** [2] 398–401 (2015).
- M. A. Wilson, et al., “Rehydroxylation of Fired-Clay Ceramics: Factors Affecting Early-Stage Mass Gain in Dating Experiments,” *Archaeometry*, **56**, 689–702 (2014).
- M. A. Wilson, W. D. Hoff, C. Hall, B. McKay, and A. Hiley, “Kinetics of Moisture Expansion in Fired Clay Ceramics: A (Time)<sup>1/4</sup> Law,” *Phys. Rev. Lett.*, **90**, 125503, 4pp (2003).
- M. A. Wilson, A. Hamilton, C. Ince, M. A. Carter, and C. Hall, “Rehydroxylation (RHX) Dating of Archaeological Pottery,” *Proc. R. Soc. A.*, **468**, 3476–93 (2012).
- S. D. Savage, M. A. Wilson, M. A. Carter, W. D. Hoff, C. Hall, and B. McKay, “Moisture Expansion and Mass Gain in Fired Clay Ceramics: A Two-Stage (Time)<sup>1/4</sup> Process,” *J. Phys. D: Appl. Phys.*, **41**, 055402, 4pp (2008).
- C. Hall, M. A. Wilson, and W. D. Hoff, “Kinetics of Long-Term Moisture Expansion in Fired-Clay Brick,” *J. Am. Ceram. Soc.*, **94**, 3651–4 (2011).
- L. O. C. Johnson, “Changes in a 50 m Mural Tape Standardising Base,” *Engineer*, **203**, 632–4 (1957).
- W. F. Cole, “Changes in a 50 m Mural Tape Standardising Base,” *Engineer*, **223**, 769–70 (1967).
- R. G. Smith, “Moisture Expansion of Structural Ceramics: V. 28 Years of Expansion,” *Brit. Ceram. Trans.*, **92**, 233–8 (1993).
- S. Zsembery, R. T. Waechter, and T. H. McNeilly, “The Expansion of Clay Bricks After 30 Years and a Method for Its Prediction”; pp. 182–91 in *Proceedings of the Seventh Australian Masonry Conference*, Newcastle, 2004.
- P. Bet, A. Fenet, and A. Counord-Monteneri, “La Typologie de la Sigillée Lisse de Lezoux. In: *Ier-IIIème s. Considérations Générales et Formes Inédites*”; Proceedings of the S.F.E.C.A.G. meeting in Lezoux, 1989.
- P. Bet, “De L’argile à la Céramique: Le Centre de Production de Lezoux à L’époque Romaine,” *Géologues*, **173**, 61–6 (2012).
- A. Blanc, “Études Techniques sur la Poterie Gallo-Romaine de Lezoux,” *Revue Archéologique du Centre*, **3**, 39–48 (1964).
- C. Ince, “Water Transport Kinetics in Mortar-Masonry Systems”; PhD Thesis (Chap. 9). The University of Manchester, Manchester, UK, 2009.
- V. A. Drits and D. K. McCarty, “The Nature of Structure-Bonded H<sub>2</sub>O in Illite and Leucophyllite from Dehydration and Dehydroxylation Experiments,” *Clays Clay Miner.*, **55** [1] 45–58 (2007).
- V. A. Drebuschak, L. N. Mylnikova, and T. N. Drebuschak, “The Mass-Loss Diagram for the Ancient Ceramics,” *J. Therm. Anal. Calorim.*, **104**, 459–66 (2011).
- F. Clegg, C. Breen, M. A. Carter, C. Ince, S. D. Savage, and M. A. Wilson, “Dehydroxylation and Rehydroxylation Mechanisms in Fired Clay Ceramics: A TG-MS and DRIFTS Investigation,” *J. Am. Ceram. Soc.*, **95**, 416–22 (2012).
- S. Lagergren, “Zur Theorie der Sogenannten Adsorption Gelöster Stoffe,” *K. Sven. Vetenskapsakad. Handl.*, **24** [4] 1–39 (1898).
- M. Vokác, A. Klouzaková, V. Hanykyr, and P. Bouska, “Dilatometric Analysis of Ceramic Roof Tiles for Determining Irreversible Moisture Expansion,” *Ceram.-Silikáty*, **53** [4] 303–9 (2009).
- S. J. Clelland, M. A. Wilson, M. A. Carter, and C. M. Batt, “RHX Dating: Measurement of the Activation Energy of Rehydroxylation for Fired-Clay Ceramics,” *Archaeometry*, doi: 10.1111/arc.12118 (2014).
- G. T. Barrett, “Rehydroxylation Dating of Fired Clays: An Improved Time-Offset Model to Account for the Effect of Cooling on Post-Reheating Mass Gain,” *J. Archaeol. Sci.*, **40**, 3596–603 (2013).
- Y. Gallet, A. Genevey, M. Le Goff, N. Warmé, J. Gran-Aymerich, and A. Lefèvre, “On the Use of Archaeology in Geomagnetism, and Vice-Versa: Recent Development in Archeomagnetism,” *C.R. Physique*, **10**, 630–48 (2009). □



### Supplementary figure S1

Fractional mass variations (fmv) in ppm at constant temperature (12.6°C) and RH% (32%) obtained for different samples of French fired-clay ceramics during their re-equilibrium after several weeks of "natural" drying (i.e. after their wet cutting) in room conditions (>60% RH, ~20°C). Red and yellow curves: samples from site Bois d'Epense -BDE01-, 1785-1815 AD; blue, pink, dark grey and light grey curves: samples from site Ancy-le-Franc -ALF03-, 1797-1807 (see in Le Goff and Gallet, 2014). The small inset shows the full-scale variations. For comparison, we also show the fmv obtained from an inert sample of SiO<sub>2</sub> (black curve) and the data from a Lezoux fragment (same collection as in Le Goff and Gallet, 2014) showing one of the smallest  $t^{1/4}$  slope after heating at 105°C (green curve).

# Supplementary Figure S2

Animation of resultant mass-gain curves derived from Equation (1) given in the text.

Same legend as for Fig. 7, except that the combination between the  $t^{1/4}$  and  $t^{1/2}$  power law processes changes from 0% to 100%.

For a best view, the following pages must be displayed in full page mode

